13 Jul 2018

Seismic Performance and Retrofit Evaluation of Hollow-Core Composite Bridge Columns

Mohanad M. Abdulazeez

Ahmed Gheni

Nicholas Colbert

Mohamed ElGawady
Missouri University of Science and Technology, elgawadym@mst.edu

SEISMIC PERFORMANCE AND RETROFIT EVALUATION OF HOLLOW-CORE COMPOSITE BRIDGE COLUMNS

Mohanad M. Abdulazeez[1]; Ahmed Gheni[2]; Nicholas Colbert[3]; and Mohamed A. ElGawady[4§], PhD, M. ASCE

[1]Graduate Research Assistance and PhD student, Dept. of Civil, Architectural, and Environmental Engineering, Missouri University of Science and Technology, Rolla, MO. 65401; Email: mma548@mst.edu
[2] PhD Candidate, Dept. of Civil, Architectural, and Environmental Engineering, Missouri University of Science and Technology, Rolla, MO. 65401; Email: aagmr6@mst.edu
[3] Graduate Research Assistance, Dept. of Civil, Architectural, and Environmental Engineering, Missouri University of Science and Technology, Rolla, MO. 65401; Email: nbcwd2@mst.edu
[4] Benavides Associate Professor, Dept. of Civil, Architectural, and Environmental Engineering, Missouri University of Science and Technology, Rolla, MO. 65401; Email: elgawadym@mst.edu
§Corresponding author

ABSTRACT: This paper presents the seismic behavior of large-scale hollow-core fiber-reinforced polymer-concrete-steel (HC-FCS) bridge column. The HC-FCS column consists of a concrete wall sandwiched between an outer fiber-reinforced polymer (FRP) tube and an inner thin-walled steel tube. The width-to-diameter ratio for the steel tube was 147. The column had an outer diameter of 24 inches and a height-to-diameter ratio of 4.0. The steel tube was embedded into reinforced concrete footing with an embedded length of 1.25 times the steel tube diameter, while the FRP tube only confined the concrete wall thickness and curtail at the top of the footing level. The column was first tested as a vertical cantilever by applying cyclic horizontal and constant axial loads to the top of the column. Then, the column was repaired using a rapid repair technique within 6 hours duration and retested under the same seismic loading condition. The retrofitting technique includes wrapping three glass FRP layers around the outer bottommost FRP tube that ruptured at the interface joint between the column and the footing during the first test. The results revealed that the HC-FCS column achieved the ductile behavior with good inelastic deformation capacity under seismic loads. While, repaired column performed relatively well under cyclic loading, recovering 34% flexural strength and 80% of the lateral displacement capacity compared to the virgin tested column.

1 INTRODUCTION

It's estimated that Americans spend 14.5 million hours per day on traffic. 10 to 15% of that congestion is caused by work zones even when it occurs in the off-peak, they increase traffic congestion [1,2]. Therefore, new bridge construction techniques are required to reduce the amount of time it takes to build our roads and bridges from months to days. Accelerated bridge construction (ABC) is a proposed technology to minimize earthquake-induced residual deformations, damage, and associated repair costs.

According to the US Federal Highway Administration, ABC is a paradigm shift where minimizing the mobility impacts of on-site and speed up the construction process. ABC includes such elements as prefabricated modular units that are built off-site in a controlled environment and then transferred to the construction area for rapid installation. ABC reduces traffic disruptions and life-cycle costs and improves construction quality and safety, resulting in more sustainable development [3]. One technique to accelerate bridge construction is to use precast bridge columns with excellent seismic performance.

Recently, interest has been rapidly growing in using fiber reinforced polymer (FRP) tubes in construction as a replacement for the outer steel tube of double skin tubular (DSTCs) column [4, 5]. The proposed column, hollow core FRP-Concrete-Steel (HC-FCS), consists of an inner steel tube and an outer FRP tube, with a concrete shell placed in-between the two tubes [Fig. 1].

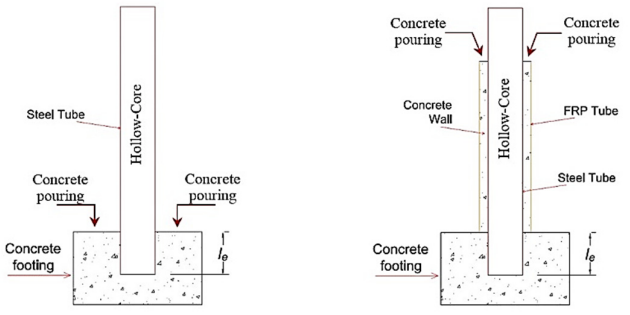

Figure 1. General arrangement of the construction of the HC-FCS column (a) inserting the steel tube and casting the footing, (b) installing the FRP tube and pouring the concrete shell

HC-FCS composite columns have several advantages as a precast element over conventional reinforced concrete or structural steel. The concrete infill is confined by both FRP and steel tubes, which results in a triaxial state of compression that increases the strength and strain capacity of the concrete infill and enhances the seismic performance of such columns [6-9]. The concrete shell reduces the susceptibility of the local and global buckling of the steel tube.

Fiber-reinforced polymer (FRP) is outstanding in its high strength-to-mass ratio, and has been used weidly for retrofitting existing structures during the past decades [10,11].

2 RESEARCH SIGNIFICANCE

The main objective of this study is to investigate the performance of HC-FCS column having thin-walled steel tube under seismic loads. The column had a steel tube diameter-to-thickness ratio (D_i/t_s) of 147. The column first tested under axial and quasi-static cyclic loads, then repaired rapidly and retested under the same loads condition.

3 EXPERIMENTAL PROGRAM

3.1 *Specimen Description*

In this study, a 0.4-scale HC-FCS column, F4-24-P1(0.8)4 was tested under constant axial load and lateral cyclic load. The F4-24-P1(0.8)4 column had a circular cross section with an outer diameter (D_f) of 24 inches and a clear height of 80 inches. The lateral load was applied at a height of 95 inches with a shear span-to-depth ratio of approximately 4.0.

The column consisted of an outer filament-wound GFRP tube with a thickness of 0.125 inches. The inner steel tube had an outer diameter of 16 inches and a thickness of 0.109 inches corresponding to inner-diameter-to-thickness D_i/t_s of 147. The steel tube was manufactured in The Highbay laboratory of Missouri University of Science and Technology by performing a seam-welding (full-penetration groove weld according to AWS 2000) for a 0.109-inches steel sheet cut and rolled to the required dimensions (length x circumference) prior to the welding. A concrete shell with a thickness of 4 inches was sandwiched between the steel and FRP tubes [Fig. 2].

The inner steel tube had yield stress of 56,240 psi, ultimate stress of 62,800 psi, yield strain of 2.15%, and an ultimate strain of 5.4%. The steel rebar had yield stress of 60,000 (psi), ultimate stress of 90,000 (psi), and ultimate strain of 0.08. The rebar properties are based on the manufacturer's data sheet while the steel tube properties were determined through tensile steel-coupon testing according to ASTM A 1067.

The used GFRP tube, was made with a matrix of Iso-polyester with a wall thickness of 0.125 inch, and based on the manufacturer's datasheet, had an axial elastic modulus of 1,400 ksi, hoop elastic modulus of 2,200 ksi, axial ultimate stress of 17,900 psi, and hoop rupture stress of 40,000 psi.

The columns' label used in the current experimental work consisted of four segments. The first segment is a letter F in reference to flexural testing, followed by the column's height-to-outer diameter ratio (H/D_f). The second segment refers to the column's outer diameter (D_f) in inches. The third segment refers to the GFRP matrix using "P" for Iso-Polyester base matrices; this is followed by the GFRP thickness in 1/8 inch, steel thickness in 1/8 inch, and concrete shell thickness in inches.

The steel tube of the column was embedded into the footing while the FRP tube truncated at the face of the footing without any embedment. The embedment depth, l_e, was determined using equation 1 [12].

$$\frac{D_i t_s F_u}{(l_e{}^2)} \leq 3.3\sqrt{f'_{c,FT}} \quad (1)$$

where D_i is the steel tube outer diameter (being 16 inches), t_s is the steel tube thickness (being 0.109 inches), and F_u is the ultimate stress of steel tube (being 62,800 psi) , and $f'_{c,FT}$ is the unconfined cylindrical compressive strength of the concrete footing (being 5,500 psi). Using these values an embedded length of 20 inches was deduced. Therefore, during the experimental work, l_e of 20 inches corresponding to 1.25 D_i (D_i is the inner diameter of the steel tube) was used to achieve the full embedment of the HC-FCS column [Fig. 1].

The concrete footing that was used in this study had a length x width x depth of 60-inches x 48-inches x 34 inches with bottom reinforcements of 7-#7, top reinforcements of 6-#7, and shear reinforcement of #4 at 2.5 inches [Fig. 2]. The steel cage of the footing was installed into the formwork.

The construction steps were as follows: 1) preparing and installing the reinforcement cages of the footings; 2) installing the steel tube into the footing cage with an embedded length of 20 inches; 3) pouring the concrete of the footing; 4) installing the GFRP tube and pouring the concrete of the concrete shell; 5) installing the reinforcement cage of the column head with dimensions of length x width x depth of 30-inches x 30- inches x 32 inches around the and concrete pouring.

Pea gravel with a maximum aggregate size of 3/8 inches was used for concrete mixtures. The unconfined concrete strengths ($f'c$) for F4-24-P1(0.8)4 at 28 days and at the day of the test were 6,305 (psi)

and 6,575 (psi) for the concrete wall, while 5,960 (psi) and 6,295 (psi) were obtained for the footing at the same ages, respectively.

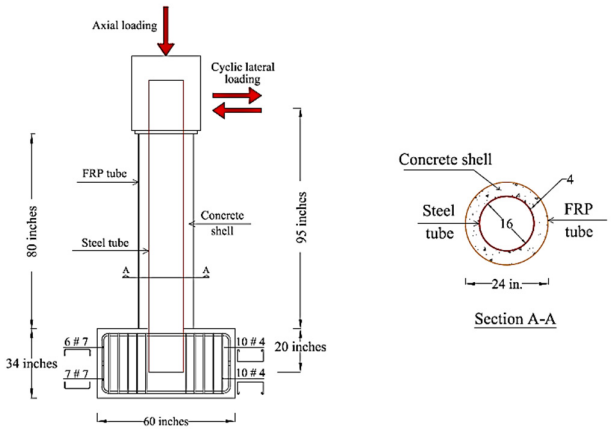

Figure 2. Construction layout of the column (a) elevation, (b) column cross-section (A-A)

3.2 *Test setup and instrumentations*

Sixteen linear variable displacement transducers (LVDTs) and string potentiometers (SPs) were assigned for measuring different displacements in each test specimen [Fig. 3 (a)]. Four LVDTs were mounted on each of the north and south faces of the column to measure the vertical displacements along the potential plastic hinge region. Two more LVDTs were attached to the footing for measuring the uplift and sliding of the footing during the test. The effects of the footing uplift and sliding were considered before calculating the lateral displacement and curvature of the column.

Forty strain gauges were installed on the FRP tube at five levels with 5 inch spacing between them. Four horizontal and four vertical strain gauges were installed at each level [Fig. 3 (b)]. Sixty-four strain gauges were installed inside the steel tube at seven levels with a spacing of 5 inches [Fig. 3 (c)]. Four horizontal and four vertical strain gauges were installed at each level. A high definition webcam was placed inside the steel tube 20 inches from the top of the footing level to film any potential buckling of the steel tube and any internal damage.

Three string Potentiometers (SPs) were assigned for measuring the slip between the FRP tube, concrete wall, and the steel tube. To achieve that, a 0.75 inches in diameter hole was drilled at hieght of 5 inches (from the top level of the footing) all the way to the steel tube [Fig. 4]. Then, the SPs were mounted in three positions : 1) on FRP tube to meaure the FRP tube, 2) connected to metal rods fixed on the concrete wall to measure it's movement, and 3) connected to metal rods fixed on the steel tube from inside (opposite to the hole from outside) throug an opening into the head to measure the relative movement at the same level (5 inches from the top level of the footing) [Fig. 4 (b)].

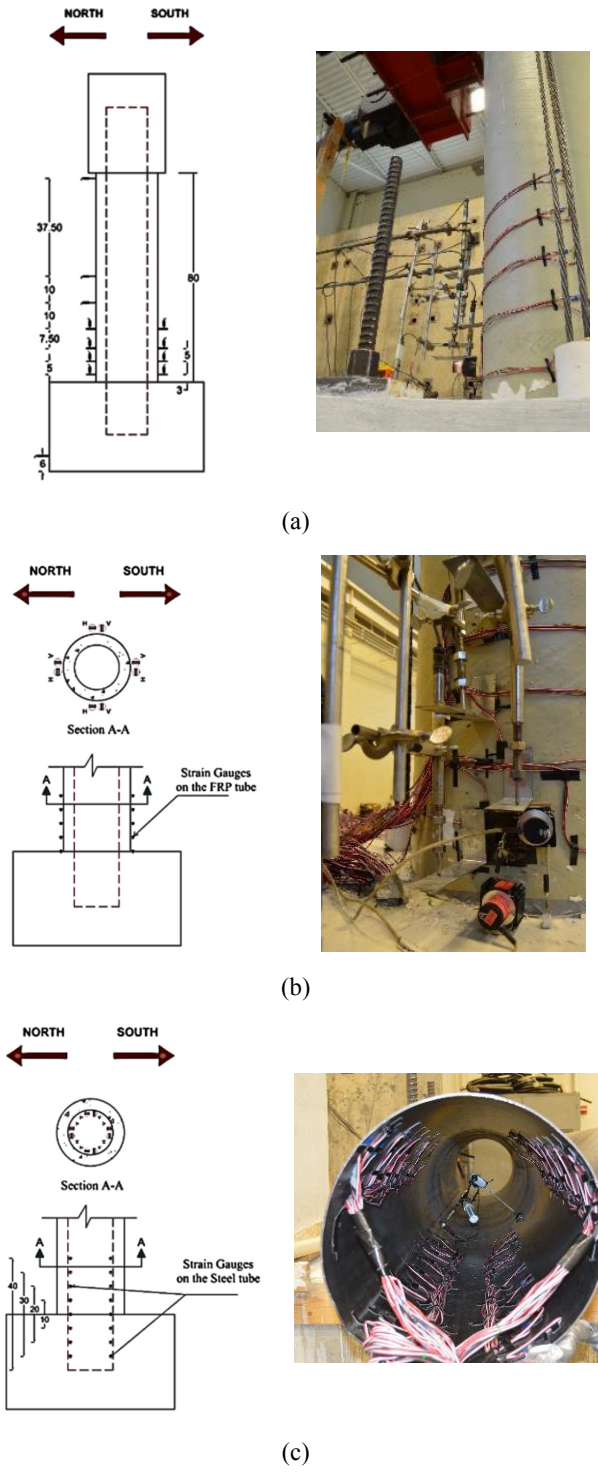

(a)

(b)

(c)

Figure 3. Strain gauges layout: (a) LVDT's and SP's installed, (b) mounted on GFRP tube, (c) mounted on steel tube

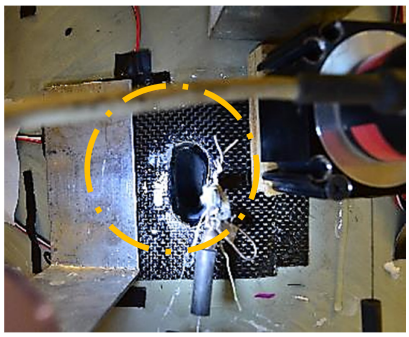

(a)

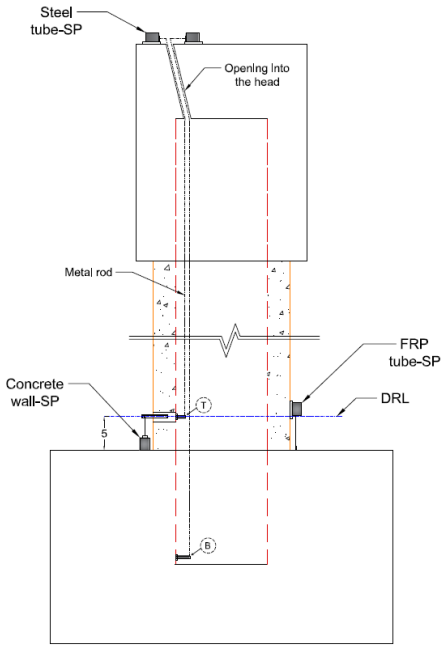

(b)

Figure 4. (a) Hole into the F4-24-P1(0.8)4 column for the relative movements measuring of the FRP tube, concrete wall, and inner steel tube, (b) hole and instrumentation layout

3.3 *Loading protocol*

Constant axial load, P, of 110 kips corresponding to 5% of the axial load capacity of the equivalent RC-column, P_o, with the same diameter and 1% longitudinal reinforcement ratio was applied to the column using six external prestressing strands [Fig. 5]. The P_o was calculated using Eq. 2 (AASHTO-LRFD 2012):

$$P_o = A_s F_y + 0.85(A_c - A_s)f'c \qquad (2)$$

where A_s = the cross-sectional area of the longitudinal steel reinforcements, A_c = the cross-sectional area of the concrete column, and F_y = the yield stress of the longitudinal steel reinforcements. The prestressing strands were supported by a rigid steel beam atop the column and the column's footing. The prestressing force was applied using two servo-controlled jacks that kept the prestressing force constant during the test.

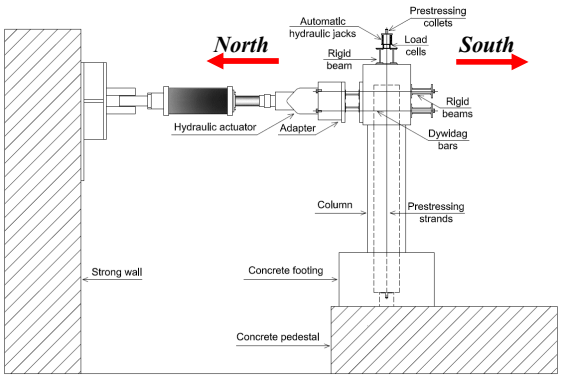

Figure 5. Layout of the test setup

After applying the axial load, a cyclic lateral load was applied in a displacement control mode using two hydraulic actuators connected to the column loading stub. The loading regime was based on the recommendations of FEMA 2007, where the displacement amplitude a_{i+1} of the step i+1 is 1.4 times the displacement amplitude of the proceeding step (a_i). Two cycles were executed for each displacement amplitude. Fig. 6 illustrates the loading regime of the cyclic lateral displacement. Each loading cycle was applied in 100 sec. corresponding to a loading rate that ranged from 0.01 inch/sec. to 0.05 inch/sec.

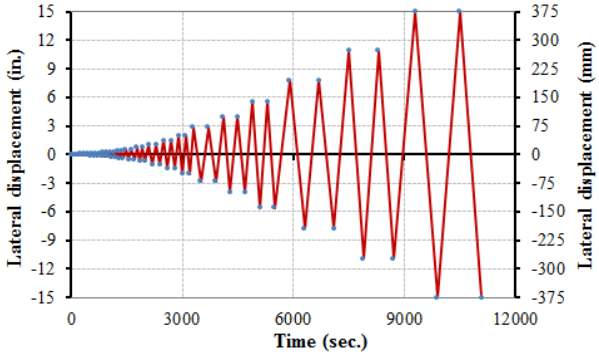

Figure 6. Lateral displacement loading regime

4 RESULTS AND DISCUSSION

Generally, the embedded length and thickness of the steel tube have significant effects on the behavior of HC-FCS columns under cyclic loads [12]. The tested column in this study had thin steel tube that was susceptible to inward buckling instabilities, and thereby steel tube slippage led to degradation of the bending strength.

Fig. 7 shows the moment drift ratio response of F4-24-P1(0.8)4 column. The lateral drift (δ) was calculated by dividing the lateral displacement measured from the actuators displacement transducers by the shear span of 95 inches. The moment (M) at the

interface joint was obtained by multiplying the force measured by the actuators' load cells by the column's height of 95 inches.

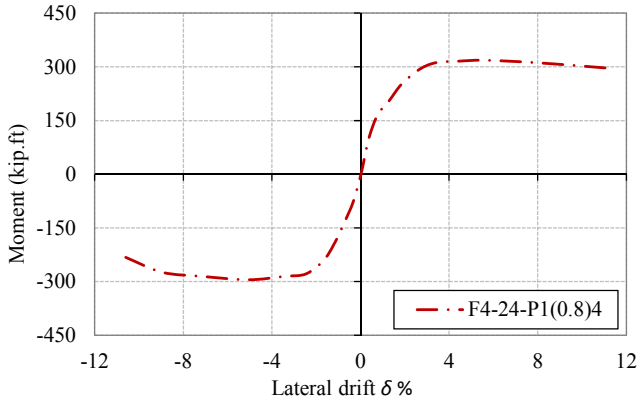

Figure 7. Moment drift ratio envelop curve

The attained moment capacity and the lateral drift were 312 kip.ft and 11.2% for column F4-24-P1(0.8)4.

Fig. 8 shows the relative movements of the FRP tube, concrete wall, and inner steel tube measured at the same level (5 inches above the interface joint, as shown in Fig. 4). As shown in the figure, at lateral drift of almost 8%, the relative movement was increased up to 1 inches between the FRP tube-concrete wall. The reason was at late lateral drift ratios, the FRP tube exhibited more lateral pressure as a result of the concrete wall dilation, and thereby, degradation of the bond interface was occurred.

While, it was in 0.6 inches at the same lateral drift between the concrete wall-steel tube indicating that the interface bond was decreased due to the steel tube local buckling. The interfacial bond failure and relative slip gradually developed at early lateral drift stage, which is related mainly to the steel tube large diameter-to-thickness ratio that influences the bond-slip performance.

Eventually, as shown in Fig. 9, the F4-24-P1(0.8)4 failed by the steel tube diamond local buckling mode of deformation followed by FRP tube rupture [Fig. 9 (b)] on the north side at 11% lateral drift.

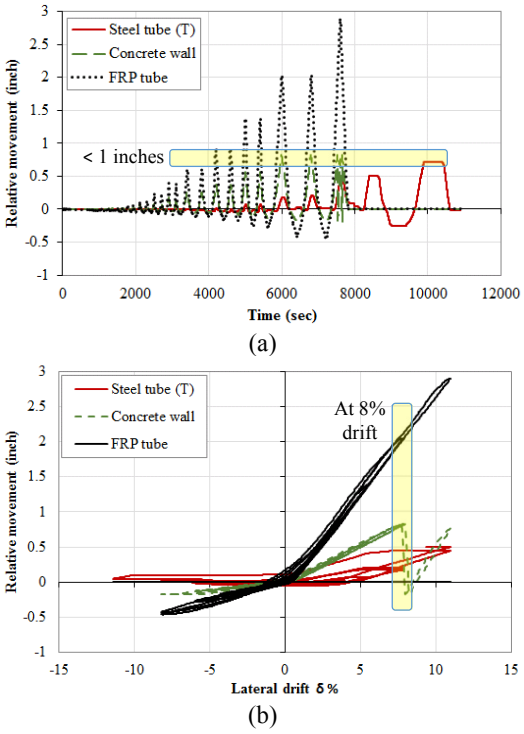

Figure 8. The relative movements of the FRP tube, concrete wall, and inner steel tube measured at 5 inches level above the interface joint (a) vs. time, (b) vs. lateral drift (%)

(a)

(b)

Figure 9. F4-24-P1(0.8)4 column (a) during the test, (b) FRP tube rupture and steel tube buckling (at 11% lateral drift)

5 RETROFITTING WORK

The economical retrofitting techniques using FRP jackets can be used to improve the seismic performance of bridge columns by increasing confinement and avoiding failures near the base of existing columns. The retrofitting schemes in this study consist of using GFRP systems, wrapped in the damaged region near the interface joint.

FRP composite jackets fabricated from GFRP by wet layup were used to rehabilitate the tested HC-FCS column. The fibers in the composite laminates were oriented in the hoop direction so that the contribution of the composites to the flexural strength of the columns was small. The composites were formed using a single sheet of GFRP with an overlap of 20 inches in the hoop direction of the columns to avoid a localized failure at the fabric ends. The jackets were started at the footing top face level and extended 40 inches above the base of the columns.

Fig. 10 illustrates the rapid repairing process of column F4-24-P1(0.8)4. The repaired column named F4-24-P1(0.8)4-R by adding the letter "R" which stands for "repair". This repairing process was selected to minimize cost of implementation for columns subjected to moderate displacement demands and was finished within 6 hours (1.5 hour GFRP wrapping, 3 hours GFRP curing, and 1.5 hour concrete mortar injection). Properties of the composite materials used in this study are listed in Table 1.

Table 1. Properties of Saturated GFRP Wrapping (Data from Fyfe Co. LLC., 2002)

Nominal thickness/layer (inches)	0.05
Young's modulus, E (ksi)	3,790
Tensile strength (ksi)	83.4
Ultimate strain	2.2%

The F4-24-P1(0.8)4-R column tested under the same lateral and axial loads that applied to the F4-24-P1(0.8)4 column. Fig. 11 shows the moment capacity versus lateral drift response of F4-24-P1(0.8)4-R column. The moment capacity and the lateral drift were 104 kip.ft and 8%, respectively (66% and 20% lower than those for column F4-24-P1(0.8)4) [Fig. 11].

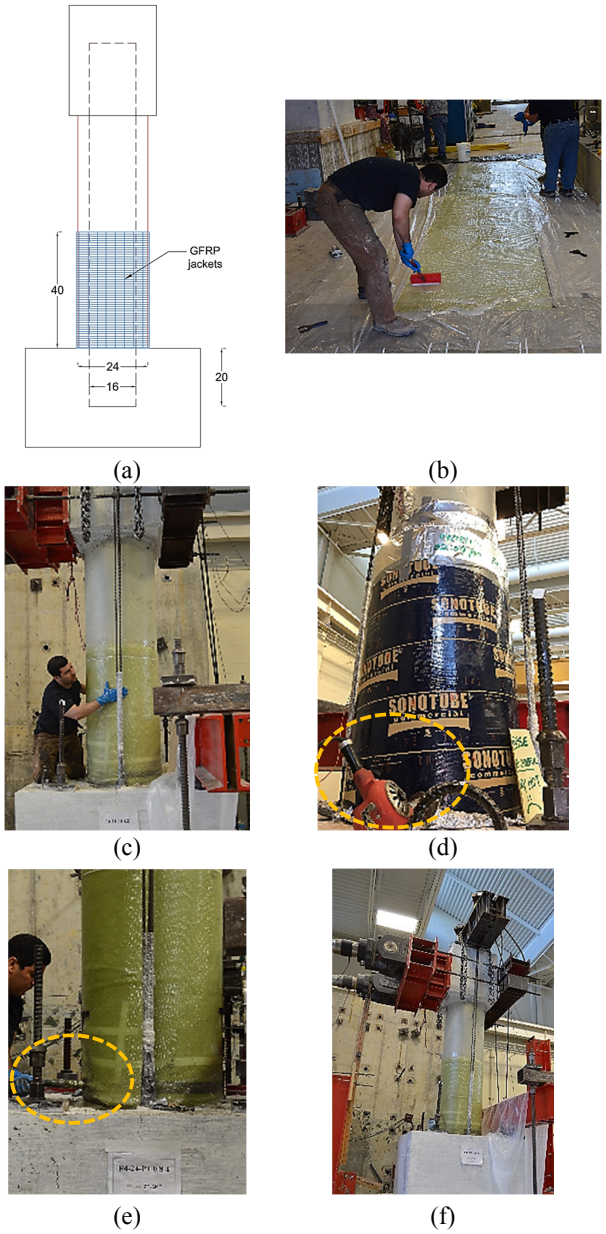

Figure 10. Retrofitting process of F4-24-P1(0.8)4 column (a) layout, (b) GFRP wet layup preparing, (c) GFRP wet layup wrapping, (d) GFRP layers curing using the heat-gun, (e) grout injecting, and (f) F4-24-P1(0.8)4-R column

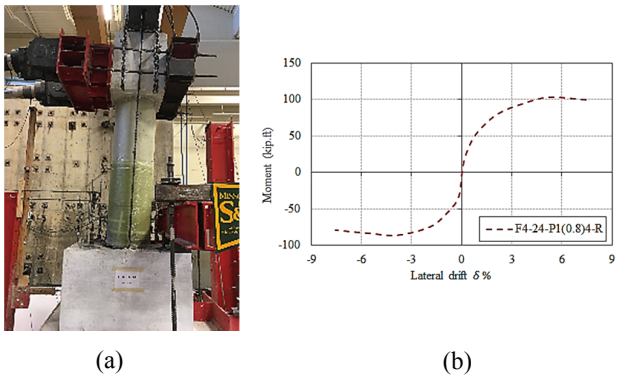

Figure 11. F4-24-P1(0.8)4-R column (a) during the test, (b) Moment drift ratio envelop curve

Careful examination of the tested column's concrete wall as well as steel tube have been conducted after peeling the FRP tube. As shown in Fig. 12 (a), the concrete wall cracked longitudinally (up to 40 inches above the footing top level) on the west side. While, it was crashed (up to 10 inches above the footing top level) on the both south and north sides where the concrete wall suffered high compression stresses. The steel tube was severely buckled locally near the footing-column interface joint [Fig. 12 (b)] as well as steel tube ductile tearing [Fig. 12 (d)], which is gradually extended 20 inches downward and upward leading to bond interface deterioration between the steel tube and the surrounding concrete. As shown in Fig. 12 (c), the end cross-section of the steel tube did not keep its circular shape. Thus, early initiation of the steel tube pull-out (slip) was observed at 2.7% lateral drift followed by bending strength dropping.

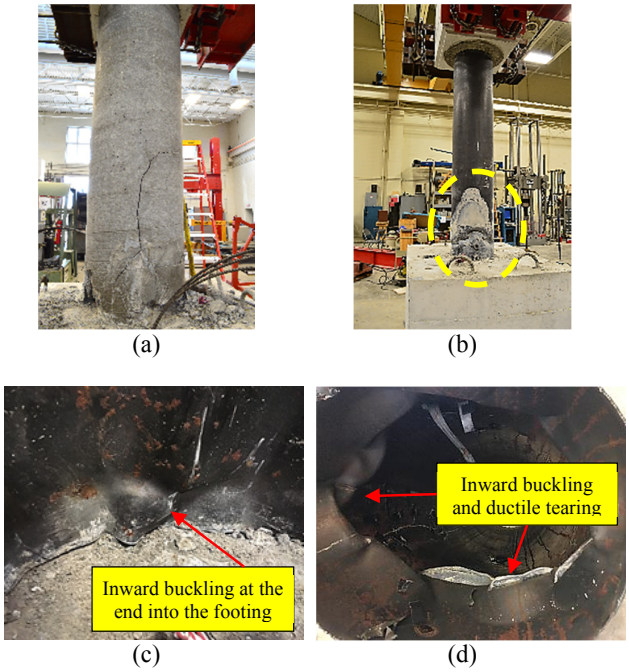

Figure 12. F4-24-P1(0.8)4-R column forensic structural (a) concrete wall cracks, (b) steel tube buckling, (c) steel tube inward buckling at the end into the footing, (b) steel tube inward buckling and ductile tearing at the interface joint

6 CONCLUSIONS

This paper presents the experimental results of a hollow-core fiber reinforced polymer concrete steel (HC-FCS) precast column. The HC-FCS column consists of a concrete hollow cylinder sandwiched between an outer fiber-reinforced polymer (FRP) tube and an inner steel tube. The column had an outer diameter of 24 inches, an inner steel tube diameter of 16 inches with D_i/t_s=147, and a height-to-diameter ratio of 4.0. The steel tube was embedded into reinforced concrete footing with an embedded length of 20 inches corresponding to 1.25 D_i, while the FRP tube acted as a formwork and provided a continuous confinement for the concrete shell, and was curtailed at the top surface of the footing. The column was subjected to constant axial load and lateral cyclic load during this study and then repaired rapidly using GRFP wet layup technique and retested under the same seismic loading regime. The tested column in this study has a thin-walled steel tube that was susceptible to inward buckling instabilities observed at small lateral drift of 2.7% led to initiate the dropping the bending strength. Therefore, steel tube slippage occurs due to the combination of the insufficient development length and the contact interface deboning with the surrounding footing and column concrete. Finally, after steel tube sever buckling at the interface joint, FRP tube rupture occurred at 11% lateral drift. The repaired column by GRFP wet layup technique displayed good lateral displacement behavior. However, the bending strength less enhanced due to the severe local buckling deformations of the inner steel tube.

7 PREFERENCES

1. Schrank, D., B. Eisele, and T. Lomax, *TTI's 2012 urban mobility report.* Texas A&M Transportation Institute. The Texas A&M University System, 2012: p. 4.
2. Schrank, D.L. and T.J. Lomax, *2009 urban mobility report*. 2009: Texas Transportation Institute, Texas A & M University.
3. Dawood, H., M. ElGawady, and J. Hewes, *Factors affecting the seismic behavior of segmental precast bridge columns.* Frontiers of Structural and Civil Engineering, 2014. 8(4): p. 388-398.
4. Teng, J. and L. Lam, *Behavior and modeling of fiber reinforced polymer-confined concrete.* Journal of structural engineering, 2004. 130(11): p. 1713-1723.
5. Teng, J., et al., *Hybrid FRP–concrete–steel tubular columns: concept and behavior.* Construction and Building Materials, 2007. 21(4): p. 846-854.
6. Abdelkarim, O.I. and M.A. ElGawady, *Analytical and Finite-Element Modeling of FRP-Concrete-Steel Double-Skin Tubular Columns.* Journal of Bridge Engineering, 2014.
7. Abdelkarim, O.I. and M.A. ElGawady, *Behavior of hollow FRP–concrete–steel columns under static cyclic axial*

compressive loading. Engineering Structures, 2016. 123: p. 77-88.

8. Abdulazeez, Mohanad M., Omar I. Abdelkarim, Ahmed Gheni, Mohamed A. ElGawady, and Greg Sanders. *Effects of Footing Connections of Precast Hollow-Core Composite Columns*. No. 17-01256. 2017.
9. Abdelkarim, O.I. and M.A. ElGawady, *Concrete-Filled-Large Deformable FRP Tubular Columns under Axial Compressive Loading.* Fibers, 2015. 3(4): p. 432-449.
10. Seible, F., et al., *Seismic retrofit of RC columns with continuous carbon fiber jackets.* Journal of composites for construction, 1997. 1(2): p. 52-62.
11. Jia, J., et al., *Cyclic load responses of GFRP-strengthened hollow rectangular bridge piers.* Advances in Materials Science and Engineering, 2014. 2014.
12. Abdelkarim, O. I., ElGawady, M. A., Gheni, A., Anumolu, S., and Abdulazeez, M. (2016). *"Seismic Performance of Innovative Hollow-Core FRP–Concrete–Steel Bridge Columns." Journal of Bridge Engineering, 04016120.*